AIP | Review of Scientific Instruments

Using stepped anvils to make even insulation layers in laser-heated diamond-anvil cell samples

Zhixue Du, Tingting Gu, Vasilije Dobrosavljevic, Samuel T. Weir, Steve Falabella, and Kanani K. M. Lee

Citation: Review of Scientific Instruments **86**, 095103 (2015); doi: 10.1063/1.4929667
View online: http://dx.doi.org/10.1063/1.4929667
View Table of Contents: http://scitation.aip.org/content/aip/journal/rsi/86/9?ver=pdfcov
Published by the AIP Publishing

Using stepped anvils to make even insulation layers in laser-heated diamond-anvil cell samples

Zhixue Du,[1] Tingting Gu,[1,a)] Vasilije Dobrosavljevic,[1] Samuel T. Weir,[2] Steve Falabella,[2] and Kanani K. M. Lee[1]
[1]*Department of Geology and Geophysics, Yale University, New Haven, Connecticut 06520, USA*
[2]*Lawrence Livermore National Laboratory, Livermore, California 94550, USA*

(Received 17 November 2014; accepted 17 August 2015; published online 1 September 2015)

We describe a method to make even insulation layers for high-pressure laser-heated diamond-anvil cell samples using stepped anvils. The method works for both single-sided and double-sided laser heating using solid or fluid insulation. The stepped anvils are used as matched pairs or paired with a flat culet anvil to make gasket insulation layers and not actually used at high pressures; thus, their longevity is ensured. We compare the radial temperature gradients and Soret diffusion of iron between self-insulating samples and samples produced with stepped anvils and find that less pronounced Soret diffusion occurs in samples with even insulation layers produced by stepped anvils. © *2015 AIP Publishing LLC.* [http://dx.doi.org/10.1063/1.4929667]

INTRODUCTION

The laser-heated diamond-anvil cell (LHDAC) is a popular tool that can maintain simultaneous high pressures (up to a few Mbar) and high temperatures (up to several 1000 K) while remaining compatible with a wide range of techniques that span the electromagnetic spectrum.[1,2] Despite its wide use over many disciplines, one of the drawbacks of this tool is the steep temperature gradients that are inherent to LHDAC samples due to the high thermal conductivity of the diamond anvils.[3–5] Temperature gradients occur both along the heating/compression axis (i.e., axial) as well as orthogonal to the heating direction (i.e., radial). To overcome the potentially steep gradients in the LHDAC, the most common technique is to use a layer of thermal insulation between the anvils and the sample,[6] which in turn is a good way to reduce Soret diffusion in LHDAC samples.[7]

Thermal insulation comes in two forms, solid and fluid, and often also behaves as a pressure medium in order to maintain quasi-hydrostatic conditions.[6,8,9] All thermal insulation layers have the common property of being electrical insulators with large band gaps. Common solid materials used as insulation include alkali halides LiF, NaCl, KCl, and KBr.[9] These are often pressed in to foils and sandwich a sample from above and below.[10] This process can be cumbersome and can lead to the gasket deforming to fill the voids where there is neither insulation nor sample. Fluid insulation materials include noble gases Ar and Ne used for their relative inertness as well as softness and are generally condensed from a gas either cryogenically or within a pressure vessel.[1] The process of loading fluid insulation layers can be tricky. The sample is usually balanced on a few grains of sample or pressure calibrant (e.g., ruby),[11] and as such, it may move during the gas loading process and either fall out of the sample chamber or become tilted between the anvils, potentially yielding insulation layers of non-uniform thickness and thus allows for uneven heating of the sample due to sample contact with the anvils or reduced thickness.

As shown in several studies, uneven insulation leads to uneven heating on both sides. A tilted sample embedded in NaCl thermal insulation is shown to be chemically heterogeneous, due to Soret diffusion.[7] Additionally, the axial temperature gradients are computed for a sample with uneven insulation layers and shown, not surprisingly, that the side with thicker insulation has smaller temperature gradients than the side with thinner insulation.[12] Likewise, temperature gradients are computed for insulation layers that differ in their thermal conductivity values.[10] The use of stepped anvils helps to mitigate these problems since we can control both the parallelism of the sample to the culets as well as the thickness.

Soret diffusion is chemical diffusion due to temperature gradients. Additionally, the Soret effect is controlled by the Z/r ratio of the respective cation, where Z is the cation charge and r is the ionic radius.[13] For cations with larger Z/r ratios (e.g., Fe, Mg, and Ca), the cation will move from hot to cold, whereas cations with smaller Z/r ratios (e.g., Si, Na, and K) will move from cold to hot.[14] This Soret effect is an especially common observation in LHDAC silicate samples (e.g., Refs. 3 and 15), due to the potentially steep inherent temperature gradients in both the axial and radial directions. Temperature gradients have been shown to be minimized through the use of insulation and coating of samples with a laser absorber.[7]

To overcome the potential problems with insulation layers, we have designed stepped anvils for making even insulation layers for LHDAC samples.

METHODS

Fabrication of stepped anvils

The stepped anvils were made by first masking the anvils using photolithography, and then plasma etching the anvils

[a)]Present address: Center for High Pressure Science and Technology Advanced Research, Shanghai 201203, China.

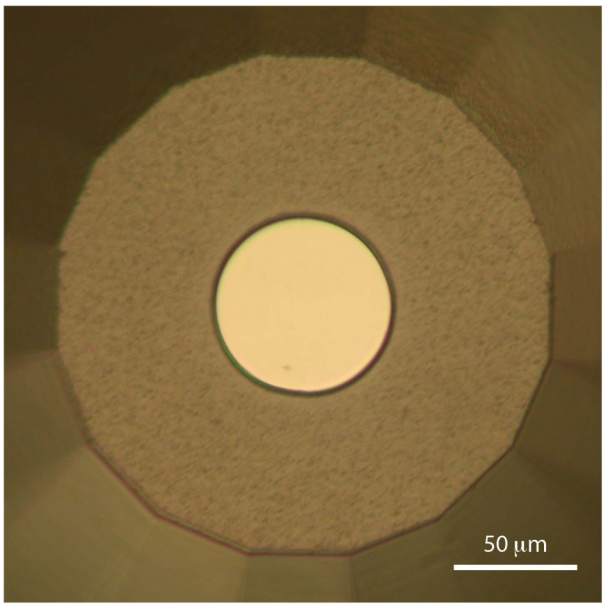

FIG. 1. Photomicrograph of stepped anvil. The culet measures 200 μm in diameter, and the step measures 70 μm in diameter with a 6 μm step height. The circular step has a shiny appearance because the tungsten mask on it has not yet been removed by acid etching.

in order to remove several micrometers of diamond from the unmasked areas. For the photolithography step, we deposited an approximately 1 μm thick layer of positive photoresist (Clariant AZ1518) onto the anvil, and then exposed the photoresist with ultraviolet light through a photolithographic mask with a projection aligner (Canon FPA-141F). The mask pattern had a clear circular opening 70 or 100 μm in diameter (for 200 and 300 μm flat culet anvils, respectively), so that only the photoresist located in a small, circular area at the center of the diamond anvil culet was exposed to UV light. After the photoresist development step, this circular area was bare of photoresist while the rest of the anvil remained masked with a thin layer of photoresist. A thin layer of tungsten about 0.5 μm thick was then sputter deposited onto the diamond anvil, and the remaining photoresist was removed using acetone. The remaining circular tungsten dot on the anvil serves as a robust mask to protect the diamond underneath it from being etched during the subsequent oxygen plasma etching step.

Oxygen plasma etching was performed with a custom designed 13.56 MHz RF-driven, hollow-cathode plasma source at Lawrence Livermore National Laboratory. In this reactive etching process, the diamond chemically reacts with

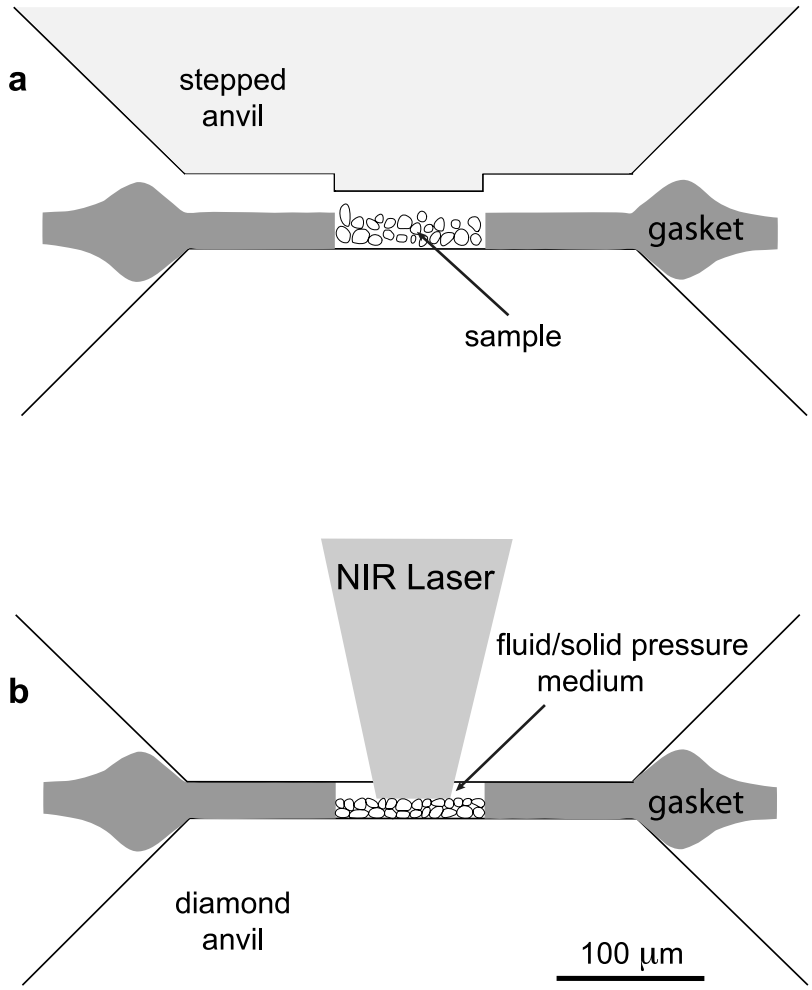

FIG. 2. Schematic of stepped anvil DAC for single-sided laser heating with fluid/solid thermal insulation layer. (a) The stepped anvil (shaded) opposes a flat anvil and used to gently compress the solid powdered sample into the pre-compressed and drilled gasket hole. (b) The gasket with the stepped anvil-pressed sample layer is loaded into a LHDAC, and thermal insulation loaded into the void left by the stepped anvil and then brought to the desired pressure. Sample is subsequently laser heated through the insulated side.

the oxygen plasma, producing volatile products (e.g., CO and CO_2), which are pumped away by the vacuum system. Further details about the plasma etching system and process can be found in Ref. 16. Attractive features of our oxygen plasma etching process are (1) that it is a relatively "gentle" method of removing diamond since the plasma uses relatively low-energy ions of about 60 eV, thus minimizing the chances of forming microcracks or other defects that might weaken the diamond anvils. Also, (2) the ion beam of our plasma etching system is highly directional, so that the features etched into the diamond anvils precisely match those of the tungsten masks. As a result, features can be precisely etched into diamond with micrometer accuracy. Figure 1 shows a photomicrograph of a completed stepped anvil.

As experiments and experimental setups vary across labs and disciplines, we describe four different configurations that can be used to cover most experiments: two are for single-sided laser heating and two for double-sided laser heating.

Single-sided LHDAC samples, fluid/solid insulation

For single-sided laser heating, only one anvil needs to be insulated from the sample. To ensure a uniform insulation layer, we equip a DAC with one stepped anvil opposite a flat culet anvil of the same size as the culets used for the LHDAC high-pressure experiment (Fig. 2(a)). We place a precompressed gasket with a centered hole the same size as the diameter of the corresponding stepped anvil, over the flat culet anvil. The sample is compressed between these two anvils and excessive material is carefully removed. Subsequently, the gasket with the stepped sample is removed and put in the LHDAC.

For loading solid insulation, we add it to the void made by the stepped anvil. Gently closing the DAC, the solid insulation

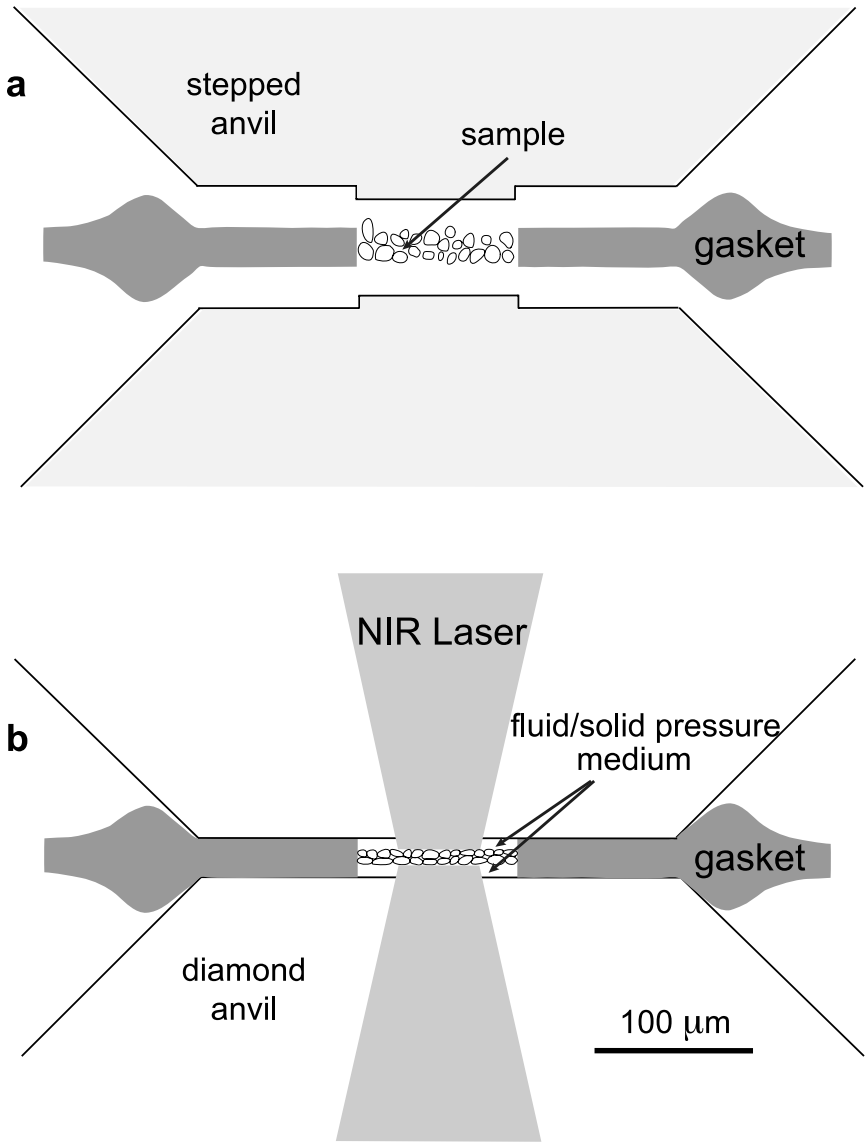

FIG. 3. Schematic of stepped anvil DAC for double-sided laser heating with fluid/solid thermal insulation layers. (a) The stepped anvils (shaded) oppose each other and are used to gently compress the solid powdered sample into the pre-compressed and drilled gasket hole. (b) The gasket with the stepped anvil-pressed sample layer is loaded into a LHDAC, and the fluid/solid thermal insulation is loaded into the voids left by the stepped anvils and brought to desired pressure. The sample is then laser heated through each insulated side.

fills the void that the stepped anvil made (Fig. 2(b)). The remaining insulation powder not within the hole is carefully removed. For fluid insulation, this can then be loaded conventionally (i.e., cryogenic or high-pressure gas loading) and fluid will simply fill the void that the stepped anvil made (Fig. 2(b)).

This ensures an even layer of insulation over the entire gasket hole that has an initial thickness identical to the stepped anvil height. Laser heating is performed on the side with the insulation layer.

Double-sided LHDAC samples, fluid/solid insulation

To ensure even insulation layers in double-sided LHDAC experiments, we equip a DAC with opposing stepped anvils (Fig. 3(a)). A precompressed gasket with a hole to match the size of the stepped anvils is placed between the stepped anvils and the powdered sample is carefully pressed into a foil, becoming fixed to the perimeter of the gasket hole by the compression. This leaves a void above and below the sample for fluid/solid insulation identical in thickness to the stepped height of the anvils. The gasket is carefully cleaned of excess sample material from both sides and placed into the LHDAC with two flat anvils.

As shown in Fig. 3(b), for loading solid insulation, similar to single-sided heating sample, a small amount of solid insulation is placed into the voids on both sides. After closing the LHDAC, the solid insulation fills the voids the stepped anvils made on each side. Then, the excessive material is carefully removed. In contrast, fluid insulation can be loaded conventionally (i.e., cryogenic or high-pressure loading) and the fluid will fill the voids that the stepped anvils made (Fig. 3(b)). This process ensures even layers of insulation over the entire gasket hole with the same initial thickness as the stepped anvil height on both sides of the sample.

EXPERIMENTS

To test out the stepped-anvil generated insulation layers, we compare three similar experimental runs. In all experiments, the starting material was a natural garnet peridotite BN-35 (e.g., Refs. 17 and 18), with composition MgO 47.5%, SiO_2 39.0%, Al_2O_3 4.4%, CaO 3.1%, and FeO 6.0%, by mol, normalized to 100%. Each sample was compressed to similar conditions: ~40 GPa and double-sided laser heated up to a peak temperature of 1650 K and 1800 K for no insulation and double-stepped thermally insulated samples, respectively, and 44 GPa and 2150 K for a single-stepped thermally insulated samples, by rastering across the sample for ~30 min for conversion to the stable crystalline phases. As this is a natural sample, compositional heterogeneities exist; thus, when laser heating, care is taken to ensure that runaway heating does not occur. In the first sample, "BN35_NI," no explicit insulation layers were used, as the sample insulates itself. The second sample, "BN35_DI," was made using double-sided stepped anvils with NaCl used as thermal insulation. For the third, "BN35_SI" was using single-sided stepped anvil, with Ar as thermal insulation on one side while the sample insulates itself on the other side.

Laser heating was performed using a SPI 100 W water-cooled fiber laser, with wavelength 1070 nm. The total laser power at peak temperature used in this study is between 40 and 50 W. The laser heating setup is identical to that used previously,[4] except the laser is split equally to heat both sides of sample with the use of a cube beam splitter (Newport 10BC16NP.9). Hot spots on each side are ~20 μm FWHM and smaller than the sample size of ~100 μm. Therefore, to convert and heat the entire sample area, we rastered the sample under the laser by moving the sample stage in the laser's focal plane for ~30 min for each experiment (e.g., Ref. 17), taking ~30 s to cover all parts of the sample once. Temperatures are also measured from both sides using multi-wavelength imaging radiometry[4] and a representative 2D temperature map was shown at the highest peak temperatures reached (Figs. 4(a)–6(a)). Only temperatures in the radial direction were measured, as axial temperature measurements were not possible, although these can be modeled and bracketed by the peak values given in the radial temperature maps.[12] Note that because the sample was rastered under the laser, all parts of the sample were heated during the rastering except near the

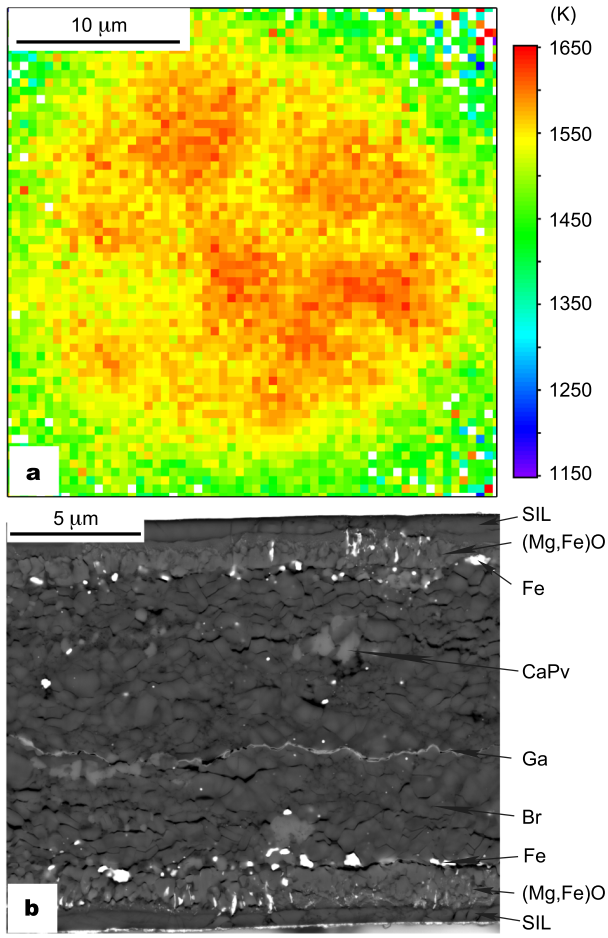

FIG. 4. (a) Representative temperature map shown for double-sided LHDAC experiment for sample BN35_NI at 40 GPa, with a peak temperature of ~1650 K. The laser was rastered across the sample for ~30 min. (b) FIB'd cross section of recovered sample. From the top to bottom are SIL, self insulation, unconverted starting material; (Mg,Fe)O, ferropericlase; Fe, iron; CaPv, calcium perovskite; Ga, gallium contamination from FIB; and Br, bridgmanite.[20] Bright spots are probably metallic iron, indicating strong Soret diffusion.

gasket edge. Peak temperatures during the heating and the temperatures measured from both sides did not vary by more than 100 K. Each sample was cut in cross section across the center of the sample using the focused ion beam (FIB)[19] in order to reveal any compositional heterogeneities produced by the temperature gradients in both axial and radial directions (Figs. 4-6).

DISCUSSION

Not unexpectedly, strong Soret diffusion of Fe is observed in the first experiment, BN35_NI. In this experiment, there are two regions where the Fe has segregated: near the top and bottom against the self-insulation layers (Fig. 4(b)). The horizontal orientation of the Fe regions is indicative of where the steep temperature gradients are, namely, along the axis of compression. Near the self-insulation layers, where it is most cool, the Fe collects.

In contrast, for the experiment BN35_DI, where sample is insulated with even NaCl layers produced by stepped anvils, the sample in cross section shows a more uniform dispersion of Fe-rich phases (Fig. 5(b)).

For the third experiment BN35_SI, laser heated from both sides, but only the top side is insulated with Ar, whereas

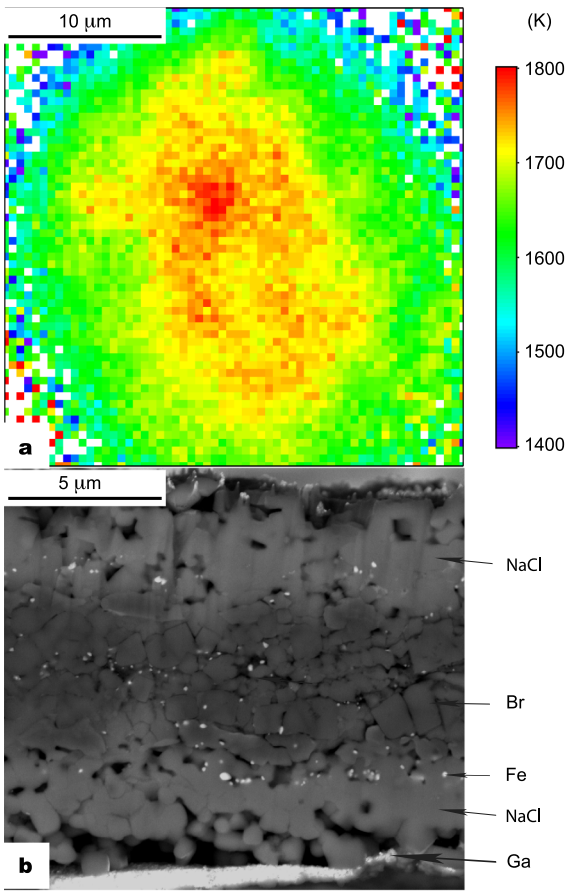

FIG. 5. (a) Representative temperature map shown for double-sided LHDAC experiment for sample BN35_DI at 41 GPa, with a peak temperature of ~1800 K. The laser was rastered across the sample for ~30 min. (b) FIB'd cross section of recovered sample. Acronyms of minerals are the same as in the caption of Fig. 4.

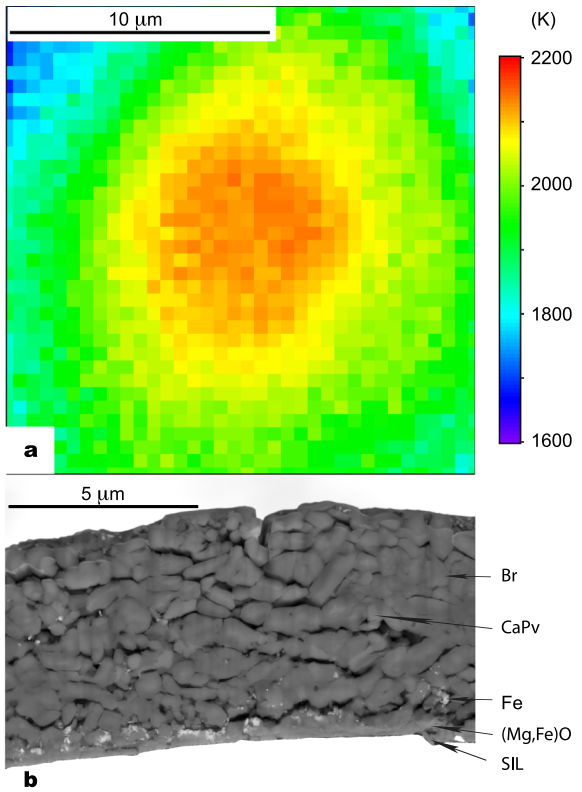

FIG. 6. (a) Representative temperature map shown for double-sided LHDAC experiment for single-sided insulated sample BN35_SI at 44 GPa, with a peak temperature of ~2150 K. The laser was rastered across the sample for ~30 min. (b) FIB'd cross section of recovered sample. Acronyms of minerals are the same as in the caption of Fig. 4.

the bottom side of the sample acts as self insulation. It is evident that the top side, with Ar insulation, where you expect a smaller axial temperature gradient, shows more uniform Fe distribution (Fig. 6(b)). This is consistent with the texture from BN35_DI (Fig. 5(b)). In contrast, on the bottom self-insulated side, the Fe-rich phases are concentrated at the bottom edge, which is a strong indication of Soret diffusion, as is shown in BN35_NI (Fig. 4(b)). In summary, in this experiment, we can see the effect of using insulation and the level of Soret diffusion where the sample was insulated by Ar (top) and where it was not (bottom).

Stepped diamond anvils are an effective way to make even insulation layers, but as no extreme pressures are being applied to form the samples in each gasket, one can imagine using alternative hard materials such as alumina Al_2O_3, cubic zirconia ZrO_2, or moissanite SiC. Additionally, other techniques such as FIB may also be used to fabricate stepped anvils, although we have not tested that method in this study.

CONCLUSIONS

We have developed a new way to easily insulate laser-heated diamond anvil cell samples through the use of stepped anvils. We find that despite larger temperature gradients due to higher temperatures, insulation layers configured using stepped anvils provide better compositional homogeneity compared to a sample that is self-insulated with minimal radial

temperature gradients. While it is possible to make insulation layers in LHDAC samples by either making foils of solid insulation or by balancing a sample in a noble gas fluid, this method provides a way to ensure even insulation layers and minimizes sample movement during sample preparation.

ACKNOWLEDGMENTS

We thank M. Rooks and F. Camino for FIB help; Z. Jiang for SEM assistance; J. Girard, G. Amulele, W. Samela, and C. Fiederlein for technical support. Facilities' use was supported by YINQE and NSF MRSEC DMR 1119826. Research carried out in part at the Center for Functional Nanomaterials, Brookhaven National Laboratory, which is supported by the U.S. Department of Energy, Office of Basic Energy Sciences, under Contract No. DE-AC02-98CH10886. This work was funded in part by NSF (Grant Nos. EAR-1321956 and EAR-0955824).

[1]A. Jayaraman, Rev. Mod. Phys. **55**(1), 65 (1983).
[2]G. J. Piermarini, *Static Compression of Energetic Materials*, edited by S. M. Peiris and G. J. Piermarini (Springer-Verlag, Berlin, 2008).
[3]D. Andrault and G. Fiquet, Rev. Sci. Instrum. **72**(2), 1283 (2001).
[4]Z. X. Du, G. Amulele, L. R. Benedetti, and K. K. M. Lee, Rev. Sci. Instrum. **84**(7), 075111 (2013).
[5]R. Jeanloz and A. Kavner, Philos. Trans. R. Soc., A **354**(1711), 1279 (1996).
[6]W. R. Panero and R. Jeanloz, Rev. Sci. Instrum. **72**(2), 1306 (2001).
[7]R. Sinmyo and K. Hirose, Phys. Earth Planet. Inter. **180**, 172 (2010).
[8]S. Klotz, J. C. Chervin, P. Munsch, and G. Le Marchand, J. Phys. D: Appl. Phys. **42**(7), 075413 (2009).
[9]I. Uts, K. Glazyrin, and K. K. M. Lee, Rev. Sci. Instrum. **84**(10), 103904 (2013).
[10]B. Kiefer and T. Duffy, J. Appl. Phys. **97**(11), 114902 (2005).
[11]R. Boehler, Rev. Geophys. **38**(2), 221, doi:10.1029/1998RG000053 (2000).
[12]E. S. G. Rainey, J. W. Hernlund, and A. Kavner, J. Appl. Phys. **114**(20), 204905 (2013).
[13]C. E. Lesher and D. Walker, Geochim. Cosmochim. Acta **50**(7), 1397 (1986).
[14]C. E. Lesher and D. Walker, in *Diffusion, Atomic Ordering and Mass Transport*, edited by J. Ganguly, S. Saxena, and S. K. Saxena (Springer Verlag, New York, 1991).
[15]D. L. Heinz and R. Jeanloz, J. Geophys. Res. **92**(B11), 11437, doi:10.1029/JB092iB11p11437 (1987).
[16]S. T. Weir, H. Cynn, S. Falabella, W. J. Evans, C. Aracne-Ruddle, D. Farber, and Y. K. Vohra, High Pressure Res. **31**(1), 191 (2011).
[17]K. K. M. Lee, B. O'Neill, W. Panero, S. Shim, L. Benedetti, and R. Jeanloz, Earth Planet. Sci. Lett. **223**(3-4), 381 (2004).
[18]C. R. Stern, S. L. Saul, M. A. Skewes, and K. Futa, in *Proceedings of Fourth International Kimberlite Conference*, edited by J. Ross (Blackwell Scientific, 1989).
[19]Z. X. Du and K. K. M. Lee, Geophys. Res. Lett. **41**(22), 8061, doi:10.1002/2014GL061954 (2014).
[20]O. Tschauner, C. Ma, J. R. Beckett, C. Prescher, V. B. Prakapenka, and G. R. Rossman, Science **346**(6213), 1100 (2014).